

2024-02-13

1 **Difference in TMPRSS2 usage by Delta and Omicron variants of SARS-CoV-2:**
2 **Implication for a sudden increase among children**

3

4 Sosuke Kakee^{1, 2}, Kyosuke Kanai¹, Akeno Tsuneki-Tokunaga¹, Keisuke Okuno², Noriyuki
5 Namba², Katsuyuki Tomita³, Hiroki Chikumi⁴, Seiji Kageyama^{1, *}

6

7 ¹Division of Virology, Department of Microbiology and Immunology, Faculty of Medicine,
8 Tottori University, 86 Nishi-cho, Yonago, 683-8503 Japan

9 ²Division of Pediatrics and Perinatology, Department of Multidisciplinary Internal Medicine,
10 Faculty of Medicine, Tottori University, 86 Nishi-cho, Yonago, 683-8503 Japan

11 ³Department of Respiratory Medicine, National Hospital Organization Yonago Medical
12 Center, Yonago 683-8518, Japan

13 ⁴Department of Infectious Diseases, 86 Nishi-cho, Yonago, 683-8503 Japan

14

15 *Correspondence to Seiji Kageyama, MD PhD

16 Division of Virology, Department of Microbiology and Immunology, Faculty of Medicine,
17 Tottori University, 86 Nishi-cho, Yonago, 683-8503 Japan

18 Tel. +81-859-38-6081

19 E-mail skageyama@tottori-u.ac.jp

20

21 ORCID Nos.

22 Kyosuke Kanai 0000-0002-7984-207X

23 Keisuke Okuno 0000-0003-1602-0527

24 Noriyuki Namba 0000-0002-3803-4500

25 Katsuyuki Tomita 0000-0002-4050-775X

26 Hiroki Chikumi 0000-0001-7325-4990

27 Seiji Kageyama 0000-0002-5220-6137

28

29 Key words (MeSH): COVID-19, SARS-CoV-2, COVID-19 Virus variants, SARS-CoV-2 delta
30 variant, SARS-CoV-2 omicron variant

31

32

2024-02-13

33 **Abstract**

34 It has been postulated from a combination of evidence that a sudden increase in COVID-19 cases
35 among pediatric patients after onset of the Omicron wave was attributed to a reduced requirement
36 for TMPRSS2-mediated entry in pediatric airways with lower expression levels of TMPRSS2.
37 Epidemic strains were isolated from the indigenous population in an area, and the levels of
38 TMPRSS2 required for Delta and Omicron variants were assessed. As a result, Delta variants
39 proliferated fully in cultures of TMPRSS2-positive Vero cells but not in TMPRSS2-negative Vero
40 cell culture (350-fold, Delta vs 9.6-fold, Omicron). There was no obvious age-dependent selection
41 of Omicron strains affected by the TMPRSS2 (9.6-fold, Adults vs. 12-fold, Children). A
42 phylogenetic tree was generated and Blast searches (up to 100 references) for the spread of strains
43 in the study area showed that each strain had almost identical homology (>99.5%) with foreign
44 isolates, although indigenous strains had obvious differences from each other. This suggested that
45 the differences had been present abroad for a long period. Therefore, the lower requirement for
46 TMPRSS2 by Omicron strains might be applicable to epidemic strains globally. In conclusion, the
47 property of TMPRSS2-independent cleavage makes Omicron proliferate with ease and allows
48 epidemics among children with fewer TMPRSS2 on epithelial surfaces of the respiratory organs.
49

2024-02-13

50 **Introduction**

51 Since COVID-19 was recognized at the end of the year 2019 [1], it spread globally within
52 several months and became a pandemic [2]. Although the pandemic continued with the
53 periodic emergence of new variants, it has become endemic in 2023. Indeed, the World Health
54 Organization (WHO) has reported that SARS-CoV-2 infections decreased in five of the six
55 WHO regions (-14% to -76%) except for the Western Pacific Region (+14%) (COVID-19
56 Epidemiological Update- 24 November 2023). Nevertheless, the WHO is still tracking several
57 lineages of Omicron variants and has identified four variants of interest: XBB.1.5, XBB.1.16,
58 EG.5 and BA.2.86. Fortunately, epidemic strains are no longer categorized as variants of
59 concern [3].

60 The Omicron wave caused a substantial increase in infections among children compared
61 with the Delta wave [4]. A study in UK reported that 117 pediatric patients were admitted
62 during the Delta wave (1 June 2021-21 December 2021) compared with 737 during the
63 Omicron wave (22 December 2021-30 September 2022), with the peak number of weekly
64 admissions being 14 for Delta and 53 for Omicron [5]. Another report from the UK
65 highlighted the increase in cases in children aged under 1 year old. The proportion of the
66 age group (<1 year) increased steeply to 42% of children admitted to hospital with COVID-
67 19 in the 4-week period (14 December 2021 to 12 January 2022) in which Omicron variants
68 were becoming dominant in the UK according to Coronavirus (COVID-19) latest insights, 30
69 March 2023 (<https://www.ons.gov.uk>). The percentage in the Omicron wave was much higher
70 than those in earlier periods: 33% of children (8 months, January to August 2020), 30% (8
71 months, September 2020 to April 2021), and 30% (8 months, May 2021 to 13 December 2021).
72 Similarly, a US cohort also suggested that the incidence rate of SARS-CoV-2 infection with
73 the Omicron variant was 6 to 8 times that of the Delta variant in children younger than 5

74 years [6].

75 There is a potential explanation for the substantial increase among children infected
76 with Omicron variants. Variants prevalent up to the period of the Delta wave were known to
77 make efficient use of transmembrane protease, serine 2 (TMPRSS2) for cell entry. However,
78 amino acid mutations in the spike protein of Omicron variants reduced the efficiency of the
79 TMPRSS2-mediated cell entry and favored the endocytosis pathway, which is a cell entry
80 pathway that does not use TMPRSS2 [7, 8]. It is also known that TMPRSS2 expression in
81 pediatric airway cells is lower than in adults. Therefore, it can be hypothesized that the
82 decreased availability of TMPRSS2 in the Omicron strain led to an increase in the number
83 of pediatric patients [9].

84 Several host-genetic factors of a gene cluster on chromosome 3 were reported to be
85 involved in the proliferation of SARS-CoV-2 in the human body [10]. The risk-associated DNA
86 segment modulated the expression of several chemokine receptors including CCR5 of SARS-
87 CoV-2 carriers [11]. Other factors, such as inborn errors of type I interferons may also be
88 involved in SARS-CoV-2 proliferation [12]. These findings suggest that it is favorable to carry
89 out the characterization of epidemic SARS-CoV-2 strains spreading among an indigenous
90 population to minimize the virus selection caused by such genetic factors.

91 In the present study, we isolated Delta and Omicron variants from patients who visited
92 two hospitals within a single city of Japan and assessed the required levels of TMPRSS2 for
93 the proliferation of these Delta and Omicron isolates to examine the cause of the sudden
94 increase in COVID-19 cases among pediatric patients immediately after the onset of the
95 Omicron wave.

2024-02-13

96 **Materials and Methods**

97 **Ethical approval.**

98 The present study was approved by the Institutional Review Board of the Faculty of
99 Medicine, Tottori University, Japan (No.20A138, October 30, 2020) and have conducted from
100 November 1, 2020, onwards. All procedures performed in studies involving human
101 participants were in accordance with the 1964 Helsinki declaration and its later amendments
102 or comparable ethical standards.

103

104 **Ethical issues including informed consent.**

105 Sample collection was carried out after obtaining informed consent from patients through
106 a website notification and/or poster presentations at the out-patient departments in two hospitals
107 ('opt-out' system). It was guaranteed that the freedom to decline participation as a research subject,
108 and refusal to participate would have no negative effect on the person, and that he/she would be
109 able to continue to receive necessary medical cares. Transparency was preserved to the patients
110 for all information and the information was ready to be discarded according to the patient will.
111 Medical records have been accessed only by selected persons on limited occasions. A guardian was
112 selected to protect human rights for a pediatric patient. Only when all the necessary conditions
113 were fulfilled as described above, patient samples were collected and shipped to the laboratory
114 anonymously.

115

116 **Patient samples and virus isolation.**

117 Nasopharyngeal swab or saliva samples were collected from SARS-CoV-2 PCR-positive
118 patients who visited Tottori University Hospital or Yonago Medical Center in Yonago city,
119 Tottori prefecture, Japan during the period from July 2021 to August 2022.

2024-02-13

120 The samples in 1 mL UTM media (Cat. 350C, Copan Japan, Kobe city, Japan) were
121 transported to our laboratory and a portion (300 μ L) was inoculated into a TMPRSS2-
122 expressing Vero cell line (VeroE6/TMPRSS2 [13], JCRB1819, JCRB Cell Bank, Suita city,
123 Osaka) and incubated at 37°C in a 5% CO₂/ 95% air atmosphere for one hour. After removing
124 the residual inoculum by washing the surface of the cells extensively, the cells were
125 maintained in Dulbecco's Modified Eagle Medium supplemented with 5% fetal bovine serum
126 and antibiotics until cytopathic effect was observed. The supernatant was stored at -80°C as
127 viral stock until further analyses.

128

129 **Infection in TMPRSS2-positive and TMPRSS2-negative cells.**

130 One day before infection, two different Vero cell lines, TMPRSS2-positive and -negative
131 Vero cells (VeroE6 cell line lacking TMPRSS2 expression: Vero76 [14], IFO50410, JCRB Cell
132 Bank), were seeded onto a 6-well plate (1.0 \times 10⁶ cells/well). Clinical isolates were inoculated
133 (1.0 \times 10⁵copies) onto the cells and incubated at 37 °C for 1 hour. The cells were washed twice
134 with phosphate-buffered saline to remove inoculated viruses in culture supernatant and
135 maintained in culture medium (2 mL per well) for 72 hours. A portion of the culture
136 supernatant (140 μ l) was collected at the indicated time points during the 72 hours culture
137 period and subjected to real-time reverse transcription-polymerase chain reaction (RT-PCR)
138 to determine the viral production levels using RNA copy number in the culture medium.

139

140 **RNA extraction, reverse Transcription, and polymerase chain reaction.**

141 Viral RNA was extracted using QIAamp Viral RNA Mini Kit (Qiagen, Tokyo, Japan) or
142 ISOSPIN Viral RNA (NIPPON GENE, Tokyo, Japan). RT-PCR and the determination of
143 cDNA sequences were performed using previously reported methods with slight

2024-02-13

144 modifications [15]. In brief, the coding regions of SARS-CoV-2 spike protein were amplified
145 by RT-PCR using a One Taq One-Step RT-PCR kit (New England BioLabs, Tokyo, Japan)
146 and a primer pair (35F: 5'-AAGGGTACTGCTGTTATGT-3', 41R: 5'-
147 AGCTGGTAATAGTCTGAAGTG-3') for first round PCR. The first-round PCR products were
148 subjected to a second round PCR with Amplitaq Gold™ 360 Master Mix (Thermo Fisher
149 Scientific, Tokyo, Japan), and M13-tailed primer pairs 35F/35R(5'-
150 TTAATAGGCGTGTGCTTAGA-3'), 36F(5'-TCAGCCTTTTCTTATGGACC-3')/36R(5'-
151 TCCAAGCTATAACGCAGC-3'), 37F(5'-TTAGAGGTGATGAAGTCAGA-3')/37R(5'-
152 TGTTCAGCCCCTATTAAACA-3'), 38F(5'-TAACCAGGTGCTGTTCTTT-3')/38R(5'-
153 CAATCATTTTCATCTGTGAGCA-3'), 39F(5'-CAGATCCATCAAAACCAAGC-3')/39R(5'-
154 GCAAGAAGACTACACCATGA-3'), 40F(5'-TCAGAGCTTCTGCTAATCTTG-3')/40R(5'-
155 GTAATTTGACTCCTTTGAGC-3'), and 41F(5'-TTGCCATAGTAATGGTGACA-
156 3')/41R(AGCTGGTAATAGTCTGAAGTG-3'). For Omicron BA5 variants, a modified primer
157 37FBA5(5'-TTAGAGGTAATGAAGTCAGC-3') was used instead of the 37F primer in the
158 second round PCR. The second round PCR products were then subjected to the sequencing
159 reactions.

160

161 **Determination of nucleotide sequences.**

162 Nucleotide sequences were determined using a BigDye Terminators v3.1 Cycle Sequence
163 kit in accordance with the manufacturer's instructions (Thermo Fisher Scientific). Isolated
164 viruses were subtyped using the sequencing results. Variants were classified into two groups
165 according to age (Adults: 16 years or older and Children: 15 years or younger). The key amino
166 acids of spike protein were analyzed in the relation to usage of TMPRSS2 and endocytosis.

167

168 **Phylogenetic analysis.**

169 The nucleotide sequences of the amplified spike region were determined using a BigDye.
170 Terminator v3.1 Cycle Sequencing kit in accordance with the manufacturer's instructions
171 (Life Technologies). M13 and PCR primers were used for the sequencing reaction. Nucleotide
172 sequences excluding the primer regions (3,822 bases encoding the spike region, 21,563-25,384
173 of Wuhan-Hu-1) were aligned with sequences obtained from the International Nucleotide
174 Sequence Database. Of 69 sequences, 20 spike sequences were determined partially, but
175 these encompassed the region (22,824-24,152 of Wuhan-Hu-1). Inspection, manual
176 modification, and evolutionary analysis of the sequences were conducted in Molecular
177 Evolutionary Genetics Analysis Version X (MEGA X). A phylogenetic tree was constructed
178 using the neighbor-joining method (1,000 bootstrap replications) in MEGA X. An estimate of
179 the mean evolutionary diversity was also conducted using MEGA X [16]. The lineage of
180 SARS-CoV-2 Omicron variant was determined using the International Nucleotide Sequence
181 Databases (<https://www.insdc.org>).

182

183 **Statistical analysis.**

184 Statistical analyses were performed using the Mann-Whitney U test and a *P*-value less
185 than 0.05 was considered statistically significant.

186

2024-02-13

187 **Results**

188 **Properties of viral isolates**

189 Delta variants were isolated from nine adults, but none were obtained from pediatric
190 patients because of extreme rarity of infections in this population. Omicron variants were
191 isolated from 38 adults and 22 from pediatric patients (Table 1). Delta variants were collected
192 from July to September 2021. Omicron variants were collected from adults from January to
193 July 2022, whereas those from pediatric patients were obtained in almost simultaneous
194 period from January to August 2022. Among the key amino acids in the spike protein of
195 SARS-CoV-2 related to the efficiency of S1/S2 and S2' cleavage, P681R was detected in all
196 analyzed Delta variants. As for the Omicron variants, H655Y, N679K, and P681H were
197 detected in all strains analyzed in the present study (Table 1).

198 Nucleotide sequences of SARS-CoV-2 spike genes of the tested samples (GenBank
199 accession numbers, LC793397-LC793465) were mostly identical to the reference strains
200 retrieved from the International Nucleotide Sequence Database using Betacoronavirus
201 BLAST (>99.63% similarity with 100 references) (Figure 1).

202

203 **Different proliferation efficiency of Delta and Omicron variants in TMPRSS2-positive and -**
204 **negative cells**

205 The amount of progeny viruses of Delta variants in supernatants was significantly
206 higher in cultures of Vero cells in the presence of TMPRSS2 at all sampling times at 24, 48
207 and 72 hours post infection (Figure 2A). Viral proliferation level is obviously higher in
208 cultures of Vero cells with TMPRSS2. However, the level became more similar in the absence
209 of TMPRSS2 (Figure 2B). As assessed at 24 hours post-infection, Delta variants were
210 produced at significantly higher levels by Vero cells in the presence of TMPRSS2 (350x)

2024-02-13

211 compared with its absence (Figure 2C, left). Contrary to the production of Delta variants,
212 Omicron variants proliferated equally in TMPRSS2-positive and -negative cell cultures (9.6x)
213 (Figure 2C, right).

214 The production levels of Omicron variants from adults and children were equivalent in
215 the culture of Vero cells with and without TMPRSS2, although it was slightly superior in
216 cultures of the cells with TMPRSS2 (Figure 3).

217

2024-02-13

218 **Discussion**

219 Nucleotide sequences of SARS-CoV-2 genes showed extremely high homology (more than
220 99.5%) with the reference strains. Although Delta variants were produced at significantly
221 higher levels from Vero cells in the presence of TMPRSS2 *in vitro*, Omicron variants
222 proliferated equally in TMPRSS2-positive and -negative cell cultures. Omicron variants from
223 adults and children produced equivalent levels in the cultures of Vero cells regardless of the
224 presence of TMPRSS2.

225 It has been reported that China has the lowest nucleotide diversity of SARS-CoV-2,
226 followed by Europe and lastly by the USA and that the difference in such diversity coincides
227 with virus transmission time order: starting in China, then Europe and finally the USA [17].
228 Although mutations have been accumulated over time, the diversity among circulating
229 strains seems very low, and SARS-CoV-2 consensus sequences were reported to be
230 indistinguishable, and they differed by 1 to 2 mutations in the rest in most of multi-infection
231 households [18]. Others reported that substitutions were concentrated in the spike protein,
232 at a rate of 0.21 amino acid residues per month [19]. Transmission efficiency depends on the
233 unique profile of intra-host viral clones [20-22]. These findings can be attributed to the
234 inherent nature of SARS-CoV-2 originated from its unique function of 3'-to-5' exoribonuclease
235 leading to high replication fidelity [23, 24]. These mutational trends were equivalent to our
236 data shown in the phylogenetic tree from the present study. Mostly identical reference
237 strains (>99.5% homology) were found among 100 strains computed in a Betacoronavirus
238 BLAST search, suggesting the imported strains spread in the study area without any
239 mutation. The profile of key amino acids in the spike protein affecting S2' cleavage was
240 identical to the reported ones [25-27]. Therefore, the properties of the Delta and Omicron
241 variants reported elsewhere is presumably applicable to the strains in the present study.

2024-02-13

242 SARS-CoV-2 uses ACE2 for entry and the serine protease TMPRSS2 for spike protein
243 priming [28]. In the present study, the properties of TMPRSS2 were highlighted and the
244 degree of requirement for the TMPRSS2 molecule was assessed using clinical strains of Delta
245 and Omicron variants. As a result, Delta variants lost the effective replication capability in
246 the absence of TMPRSS2, but Omicron variants did not lose it. The Delta variant-specific
247 dependence on the TMPRSS2 function was prevalent for the epidemic strains, as estimated
248 in a model study [7]. TMPRSS2-dependent Delta variants have rarely infected children
249 because of the lower expression of TMPRSS2 in their airway [9]. However, Omicron variants
250 do not need enzymatic cleavage by TMPRSS2 for the replication. Independency of TMPRSS2
251 in Omicron variants is applicable to the strains from adults and children. Clinical isolates
252 derived from adult and children grew equally in Vero cells regardless of the presence of
253 TMPRSS2.

254 It has been proposed that Delta variants predominantly use TMPRSS2 for the cleavage
255 at a S2' site of the SARS-CoV-2 spike protein as compared with Omicron variants, although
256 both Delta and Omicron variants required membrane fusion for the viral replication via the
257 fusion peptide revealed by TMPRSS2 and/or Cathepsin L-mediated cleavage [7, 8, 28]. As
258 expected, the predominant usage of TMPRSS2 by Delta variants was confirmed in the
259 present study using clinical isolates from an indigenous population with similar genetic
260 backgrounds. TMPRSS2-independent cleavage allows Omicron variants to proliferate with
261 ease in children possessing lower levels of TMPRSS2 on epithelial surfaces of the respiratory
262 organs [9].

263 This study was carried out at one site only and handled a limited number of samples.
264 Similar studies are required at other sites to confirm the trends described in the present
265 study. We failed in the sampling of Delta variants from pediatric patients because of rare

2024-02-13

266 infections caused by Delta variants in the study field. Therefore, the difference in the usage
267 of TMPRSS2 by Delta and Omicron variants could not be examined directly using samples
268 from pediatric patients.

269

270 **Conclusion**

271 Analysis of epidemic strains from indigenous populations with similar genetic backgrounds
272 in one area showed that the Omicron variants were able to replicate independently in
273 pediatric patients with lower levels of TMPRSS2 on epithelial surface of the respiratory.

274

275 **Acknowledgments**

276 The authors are grateful to the patients who agreed to participate in this study and to
277 Dr. Perdana WY for technical assistance.

278

279 **Funding**

280 This work was supported in part by a Grant-in-Aid for Scientific Research on Infection
281 Control and Prevention by the International Platform for Dryland Research and Education,
282 Tottori University.

283

284 **Conflict of interest.**

285 The authors report no declarations of interest.

286

287

288 **Legends to Figures**

289 **Figure 1.** Phylogenetic tree of SARS-CoV-2 clinical isolates.

290 The phylogenetic tree was generated from the SARS-CoV-2 spike protein coding region.
291 Isolates from adults (≥ 20 years, ●) and children (≤ 14 years, ○) (GenBank accession numbers,
292 LC793397-LC793465) are shown with reference strains (▲). The reference strains with the
293 greatest distances from the present isolates were selected from the result of BLAST searches
294 of 100 beta-coronavirus sequences in the International Nucleotide Sequence Databases. The
295 scale shown the genetic distance. Wuhan-Hu-1 (NC_045512) was used as the outgroup.

296

297 **Figure 2.** Proliferation efficiency of the Delta and Omicron variants from adult patients in
298 TMPRSS2-positive or -negative Vero cells.

299 (A) The production levels of Delta variants (n=3, GenBank accession numbers, LC793397-
300 LC793399) were determined by SARS-CoV-2 genomic RNA copy number in culture
301 supernatants and compared between TMPRSS2-positive (●) and -negative (○) Vero cell
302 cultures up to 72 hours. Data plots are shown as mean \pm SD from three independent
303 experiments. (B) The levels of Omicron variants (n=3, LC793430-LC793432) were also
304 compared similarly. (C) Means and distributions of the production levels of Delta (n=6,
305 LC793397-LC793400, LC793404, LC793405) and Omicron variants (n=24, LC793430-
306 LC793442, LC793444-LC793452, LC793455, LC793456) in the supernatants of TMPRSS2-
307 positive (P) or -negative (N) Vero cell culture at 24 hours post-infection are shown as box-
308 and-whisker plots. The levels of P and N were compared among Delta/Adult and
309 Omicron/Adult isolates and showed significant difference ($P < 0.05$, Mann-Whitney U test).

310

2024-02-13

311 **Figure.3** Proliferation efficiency of Omicron variant clinical isolates from adult or pediatric
312 patients in TMPRSS2-positive or -negative Vero cells.

313 (A) The production levels of Omicron variants from adults (n=3, GenBank accession numbers,
314 LC793430-LC793432) were determined similarly in TMPRSS2 positive (●) or negative (○)
315 Vero cell culture as shown in Figure 2. (B) The levels of Omicron variants from children (n=3,
316 LC793408-LC793410) were also assessed in the same manner. (C) Means and distributions
317 of the production of Omicron variants from adults (n=24, LC793430-LC793442, LC793444-
318 LC793452, LC793455, LC793456) and pediatric patients (n=21, LC793408-LC793415,
319 LC793417-LC793429) in the supernatants of TMPRSS2-positive (P) or negative (N) Vero cell
320 cultures at 24 hours post-infection are shown as box-and-whisker plots. No significant
321 difference was detected between the values of P and N in omicron/adults and
322 omicron/children (Mann-Whitney U test).

323

324

325 **References**

- 326 1. Zhu N, Zhang D, Wang W, Li X, Yang B, Song J, et al. A Novel Coronavirus from Patients
327 with Pneumonia in China, 2019. *N Engl J Med.* 2020;382(8):727-33. Epub 2020/01/25. doi:
328 10.1056/NEJMoa2001017. PubMed PMID: 31978945; PubMed Central PMCID:
329 PMCPMC7092803.
- 330 2. Estimating excess mortality due to the COVID-19 pandemic: a systematic analysis of
331 COVID-19-related mortality, 2020-21. *Lancet.* 2022;399(10334):1513-36. Epub 2022/03/14.
332 doi: 10.1016/s0140-6736(21)02796-3. PubMed PMID: 35279232; PubMed Central PMCID:
333 PMCPMC8912932.
- 334 3. Telenti A, Hodcroft EB, Robertson DL. The Evolution and Biology of SARS-CoV-2
335 Variants. *Cold Spring Harb Perspect Med.* 2022;12(5). Epub 2022/04/22. doi:
336 10.1101/cshperspect.a041390. PubMed PMID: 35444005; PubMed Central PMCID:
337 PMCPMC9159258.
- 338 4. Koelle K, Martin MA, Antia R, Lopman B, Dean NE. The changing epidemiology of
339 SARS-CoV-2. *Science.* 2022;375(6585):1116-21. Epub 2022/03/11. doi:
340 10.1126/science.abm4915. PubMed PMID: 35271324; PubMed Central PMCID:
341 PMCPMC9009722.
- 342 5. Cheng DR, Schrader S, McMinn A, Crawford NW, Tosif S, McNab S, et al. Paediatric
343 admissions with SARS-CoV-2 during the Delta and Omicron waves: an Australian single-
344 centre retrospective study. *BMJ Paediatr Open.* 2023;7(1). Epub 2023/03/08. doi:
345 10.1136/bmjpo-2023-001874. PubMed PMID: 36882231; PubMed Central PMCID:
346 PMCPMC10008196.
- 347 6. Wang L, Berger NA, Kaelber DC, Davis PB, Volkow ND, Xu R. Incidence Rates and
348 Clinical Outcomes of SARS-CoV-2 Infection With the Omicron and Delta Variants in
349 Children Younger Than 5 Years in the US. *JAMA Pediatr.* 2022;176(8):811-3. Epub
350 2022/04/02. doi: 10.1001/jamapediatrics.2022.0945. PubMed PMID: 35363246; PubMed
351 Central PMCID: PMCPMC8976262.
- 352 7. Meng B, Abdullahi A, Ferreira I, Goonawardane N, Saito A, Kimura I, et al. Altered
353 TMPRSS2 usage by SARS-CoV-2 Omicron impacts infectivity and fusogenicity. *Nature.*
354 2022;603(7902):706-14. Epub 2022/02/02. doi: 10.1038/s41586-022-04474-x. PubMed PMID:
355 35104837; PubMed Central PMCID: PMCPMC8942856.
- 356 8. Jackson CB, Farzan M, Chen B, Choe H. Mechanisms of SARS-CoV-2 entry into cells.
357 *Nat Rev Mol Cell Biol.* 2022;23(1):3-20. Epub 2021/10/07. doi: 10.1038/s41580-021-00418-x.
358 PubMed PMID: 34611326; PubMed Central PMCID: PMCPMC8491763.
- 359 9. Schuler BA, Habermann AC, Plosa EJ, Taylor CJ, Jetter C, Negretti NM, et al. Age-
360 determined expression of priming protease TMPRSS2 and localization of SARS-CoV-2 in lung

2024-02-13

- 361 epithelium. *J Clin Invest.* 2021;131(1). Epub 2020/11/13. doi: 10.1172/jci140766. PubMed
362 PMID: 33180746; PubMed Central PMCID: PMCPMC7773394.
- 363 10. Zeberg H, Pääbo S. The major genetic risk factor for severe COVID-19 is inherited from
364 Neanderthals. *Nature.* 2020;587(7835):610-2. Epub 2020/10/01. doi: 10.1038/s41586-020-
365 2818-3. PubMed PMID: 32998156.
- 366 11. Zeberg H. The major genetic risk factor for severe COVID-19 is associated with
367 protection against HIV. *Proc Natl Acad Sci U S A.* 2022;119(9). Epub 2022/02/24. doi:
368 10.1073/pnas.2116435119. PubMed PMID: 35193979; PubMed Central PMCID:
369 PMCPMC8892305.
- 370 12. Zhang Q, Bastard P, Cobat A, Casanova JL. Human genetic and immunological
371 determinants of critical COVID-19 pneumonia. *Nature.* 2022;603(7902):587-98. Epub
372 2022/01/29. doi: 10.1038/s41586-022-04447-0. PubMed PMID: 35090163; PubMed Central
373 PMCID: PMCPMC8957595.
- 374 13. Matsuyama S, Nao N, Shirato K, Kawase M, Saito S, Takayama I, et al. Enhanced
375 isolation of SARS-CoV-2 by TMPRSS2-expressing cells. *Proc Natl Acad Sci U S A.*
376 2020;117(13):7001-3. Epub 2020/03/14. doi: 10.1073/pnas.2002589117. PubMed PMID:
377 32165541; PubMed Central PMCID: PMCPMC7132130.
- 378 14. Nao N, Sato K, Yamagishi J, Tahara M, Nakatsu Y, Seki F, et al. Consensus and
379 variations in cell line specificity among human metapneumovirus strains. *PLoS One.*
380 2019;14(4):e0215822. Epub 2019/04/24. doi: 10.1371/journal.pone.0215822. PubMed PMID:
381 31013314; PubMed Central PMCID: PMCPMC6478314.
- 382 15. Moniruzzaman M, Hossain MU, Islam MN, Rahman MH, Ahmed I, Rahman TA, et al.
383 Coding-Complete Genome Sequence of SARS-CoV-2 Isolate from Bangladesh by Sanger
384 Sequencing. *Microbiol Resour Announc.* 2020;9(28). Epub 2020/07/11. doi:
385 10.1128/mra.00626-20. PubMed PMID: 32646908; PubMed Central PMCID:
386 PMCPMC7348026.
- 387 16. Kumar S, Stecher G, Li M, Knyaz C, Tamura K. MEGA X: Molecular Evolutionary
388 Genetics Analysis across Computing Platforms. *Mol Biol Evol.* 2018;35(6):1547-9. Epub
389 2018/05/04. doi: 10.1093/molbev/msy096. PubMed PMID: 29722887; PubMed Central
390 PMCID: PMCPMC5967553.
- 391 17. Chen YH, Wang H. Exploring Diversity of COVID-19 Based on Substitution Distance.
392 *Infect Drug Resist.* 2020;13:3887-94. Epub 2020/11/06. doi: 10.2147/idr.S277620. PubMed
393 PMID: 33149633; PubMed Central PMCID: PMCPMC7605616.
- 394 18. Bendall EE, Paz-Bailey G, Santiago GA, Porucznik CA, Stanford JB, Stockwell MS, et
395 al. SARS-CoV-2 Genomic Diversity in Households Highlights the Challenges of Sequence-
396 Based Transmission Inference. *mSphere.* 2022;7(6):e0040022. Epub 2022/11/16. doi:

2024-02-13

- 397 10.1128/msphere.00400-22. PubMed PMID: 36377913; PubMed Central PMCID:
398 PMCPMC9769559.
- 399 19. Lou J, Zhao S, Cao L, Zheng H, Chen Z, Chan RWY, et al. Temporal Patterns in the
400 Evolutionary Genetic Distance of SARS-CoV-2 during the COVID-19 Pandemic. *Public*
401 *Health Genomics*. 2022;1-4. Epub 2022/01/06. doi: 10.1159/000520837. PubMed PMID:
402 34986485.
- 403 20. Braun KM, Moreno GK, Wagner C, Accola MA, Rehrauer WM, Baker DA, et al. Acute
404 SARS-CoV-2 infections harbor limited within-host diversity and transmit via tight
405 transmission bottlenecks. *PLoS Pathog*. 2021;17(8):e1009849. Epub 2021/08/24. doi:
406 10.1371/journal.ppat.1009849. PubMed PMID: 34424945; PubMed Central PMCID:
407 PMCPMC8412271.
- 408 21. Valesano AL, Rumfelt KE, Dimcheff DE, Blair CN, Fitzsimmons WJ, Petrie JG, et al.
409 Temporal dynamics of SARS-CoV-2 mutation accumulation within and across infected hosts.
410 *PLoS Pathog*. 2021;17(4):e1009499. Epub 2021/04/08. doi: 10.1371/journal.ppat.1009499.
411 PubMed PMID: 33826681; PubMed Central PMCID: PMCPMC8055005.
- 412 22. Tonkin-Hill G, Martincorena I, Amato R, Lawson ARJ, Gerstung M, Johnston I, et al.
413 Patterns of within-host genetic diversity in SARS-CoV-2. *Elife*. 2021;10. Epub 2021/08/14.
414 doi: 10.7554/eLife.66857. PubMed PMID: 34387545; PubMed Central PMCID:
415 PMCPMC8363274.
- 416 23. Bouvet M, Lugari A, Posthuma CC, Zevenhoven JC, Bernard S, Betzi S, et al.
417 Coronavirus Nsp10, a critical co-factor for activation of multiple replicative enzymes. *J Biol*
418 *Chem*. 2014;289(37):25783-96. Epub 2014/07/31. doi: 10.1074/jbc.M114.577353. PubMed
419 PMID: 25074927; PubMed Central PMCID: PMCPMC4162180.
- 420 24. Liu C, Shi W, Becker ST, Schatz DG, Liu B, Yang Y. Structural basis of mismatch
421 recognition by a SARS-CoV-2 proofreading enzyme. *Science*. 2021;373(6559):1142-6. Epub
422 2021/07/29. doi: 10.1126/science.abi9310. PubMed PMID: 34315827; PubMed Central
423 PMCID: PMCPMC9836006.
- 424 25. Hu B, Chan JF, Liu H, Liu Y, Chai Y, Shi J, et al. Spike mutations contributing to the
425 altered entry preference of SARS-CoV-2 omicron BA.1 and BA.2. *Emerg Microbes Infect*.
426 2022;11(1):2275-87. Epub 2022/08/31. doi: 10.1080/22221751.2022.2117098. PubMed PMID:
427 36039901; PubMed Central PMCID: PMCPMC9542985.
- 428 26. Beaudoin CA, Pandurangan AP, Kim SY, Hamaia SW, Huang CL, Blundell TL, et al. In
429 silico analysis of mutations near S1/S2 cleavage site in SARS-CoV-2 spike protein reveals
430 increased propensity of glycosylation in Omicron strain. *J Med Virol*. 2022;94(9):4181-92.
431 Epub 2022/05/17. doi: 10.1002/jmv.27845. PubMed PMID: 35575289; PubMed Central
432 PMCID: PMCPMC9348480.

2024-02-13

- 433 27. Khatri R, Siddqui G, Sadhu S, Maithil V, Vishwakarma P, Lohiya B, et al. Intrinsic
434 D614G and P681R/H mutations in SARS-CoV-2 VoCs Alpha, Delta, Omicron and viruses
435 with D614G plus key signature mutations in spike protein alters fusogenicity and infectivity.
436 *Med Microbiol Immunol.* 2023;212(1):103-22. Epub 2022/12/31. doi: 10.1007/s00430-022-
437 00760-7. PubMed PMID: 36583790; PubMed Central PMCID: PMCPMC9801140.
- 438 28. Hoffmann M, Kleine-Weber H, Schroeder S, Krüger N, Herrler T, Erichsen S, et al.
439 SARS-CoV-2 Cell Entry Depends on ACE2 and TMPRSS2 and Is Blocked by a Clinically
440 Proven Protease Inhibitor. *Cell.* 2020;181(2):271-80.e8. Epub 2020/03/07. doi:
441 10.1016/j.cell.2020.02.052. PubMed PMID: 32142651; PubMed Central PMCID:
442 PMCPMC7102627.
- 443

Figure 1



Figure 2

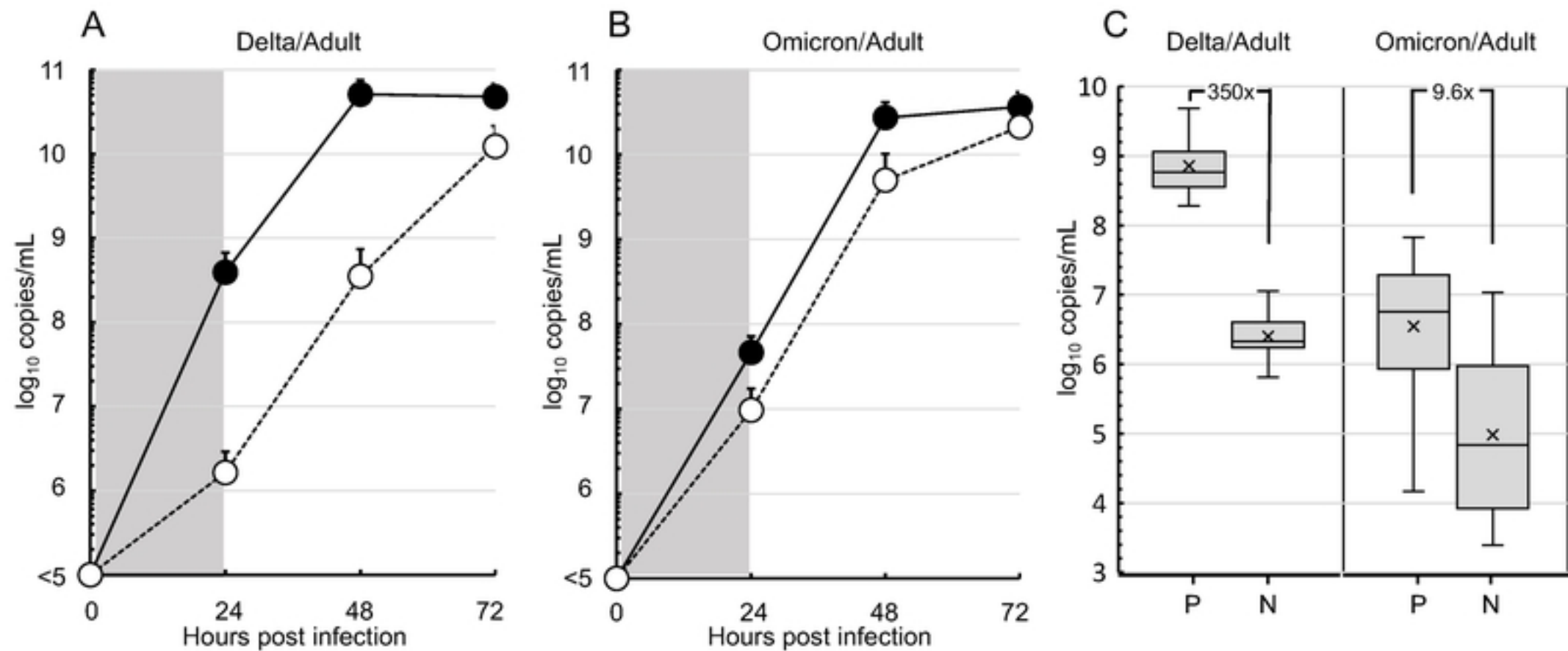


Figure 3

